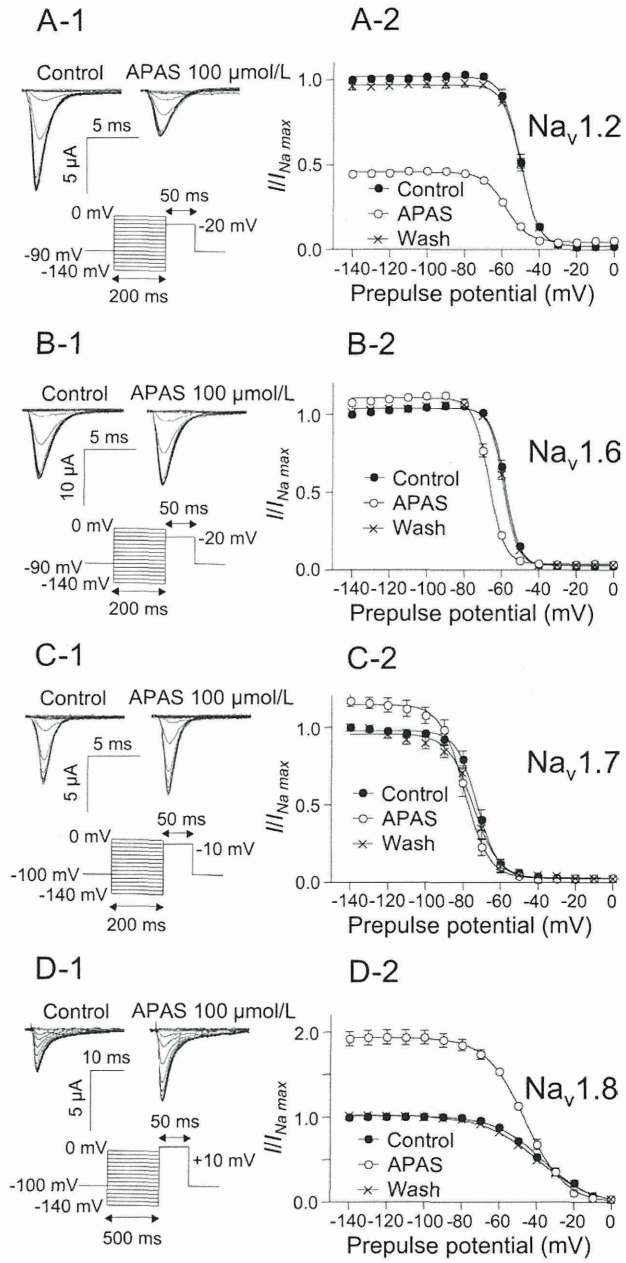

Fig. 7. Effects of allopregnanolone sulfate (APAS) on inactivation curves in oocytes expressing $Na_v1.2$ (*A*) (n = 6), $Na_v1.6$ (*B*) (n = 7), $Na_v1.7$ (*C*) (n = 5), or $Na_v1.8$ (*D*) (n = 6) α subunits with β_1 subunits. Currents were elicited by a 50-ms test pulse to −20 mV for $Na_v1.2$ and $Na_v1.6$, −10 mV for $Na_v1.7$, and +10 mV for $Na_v1.8$ after 200 ms (500 ms for only $Na_v1.8$) prepulses ranging from −140 mV to 0 mV in 10-mV increments from a V_{max} holding potential. Representative I_{Na} traces in both the absence and presence of APAS are shown in *A-1*, *B-1*, *C-1*, and *D-1*. Effects of APAS on inactivation curves (*closed circles*, control; open circles, neurosteroids; cross, washout) are shown in *A-2*, *B-2*, *C-2*, and *D-2*. Steady-state inactivation curves were fitted to the Boltzmann equation, and the $V_{1/2}$ values are shown in table 2. Data are expressed as means ± SEM. Na_v = voltage-gated sodium channel; Wash = washout.

sodium currents in the hyperpolarizing range of the inactivation curve, indicating that resting channel block is an important mechanism of APAS inhibition for only $Na_v1.2$. Both compounds demonstrated use-dependency for inhibition of $Na_v1.2$, $Na_v1.6$, and $Na_v1.7$, suggesting the ability to slow the recovery time from inactivation.[33] Many investigators have shown that sodium channel blockers, including local anesthetics, tricyclic antidepressants, and volatile anesthetics, enhance steady-state inactivation with no effect on activation and exhibit use-dependent block.[34–36] We demonstrated that APAS enhances inactivation and shows use-dependent block similar to other sodium channel blockers, yet it also has diverse effects on activation according to differences in α subunits. These actions suggest that APAS may have different binding sites or allosteric conformational mechanisms to change sodium channel function, although further investigation with site-directed mutagenesis is needed to rule out nonspecific membrane effects. PAS may have common binding sites with APAS, because it shows similar effects, although these changes were small.

The α subunit consists of four homologous domains (I to IV) containing six transmembrane segments (S1 to S6), and one reentrant P-region connecting S5 to S6 (SS1/SS2). Tetrodotoxin-sensitive α subunits, $Na_v1.2$, $Na_v1.6$, and $Na_v1.7$, are phylogenetically related and show 70 to 80% amino acid sequence identity. In contrast, tetrodotoxin-resistant α subunits, $Na_v1.8$, are phylogenetically distant and show only 55 to 56% sequence identity to the other three α subunits. In addition, the lengths of amino acid sequences of four α subunits differed within the range of 1957 to 2005 residues. Therefore, these differences would result in the diversity in neurosteroid action, especially in the effects on channel activation. Indeed, the longest extracellular regions in the α subunit (IS5 to SS1) are 93, 77, 73, and 66 amino acid residues in $Na_v1.2$, $Na_v1.6$, $Na_v1.7$, and $Na_v1.8$, respectively. The diversity in sequence and differences in the effects on activation according to α subunit may be important for clarifying binding sites and the mechanism of $Na_v1.2$ inhibition by APAS in further investigations.

γ-Aminobutyric acid type A receptors have been considered to be important for the analgesic effects of allopregnanolone because it has high potency as a positive $GABA_A$ modulator compared with other neurosteroids. Pregnanolone also affects $GABA_A$ receptors in a manner similar to that of allopregnanolone; nevertheless, its analgesic effect is weak. In fact, pregnanolone was shown to reduce mechanical allodynia without reduction of thermal heat hyperalgesia in a neuropathic pain model in contrast to attenuation of both by allopregnanolone.[28] The investigators suggested that the partial analgesic effects of pregnanolone are caused by suppression of glycine receptors by demonstrating that pregnanolone had a significant analgesic effect only in animals displaying a strychnine-induced allodynia in two types of allodynia models induced by bicuculline and strychnine.[28] Moreover, a recent report demonstrated that

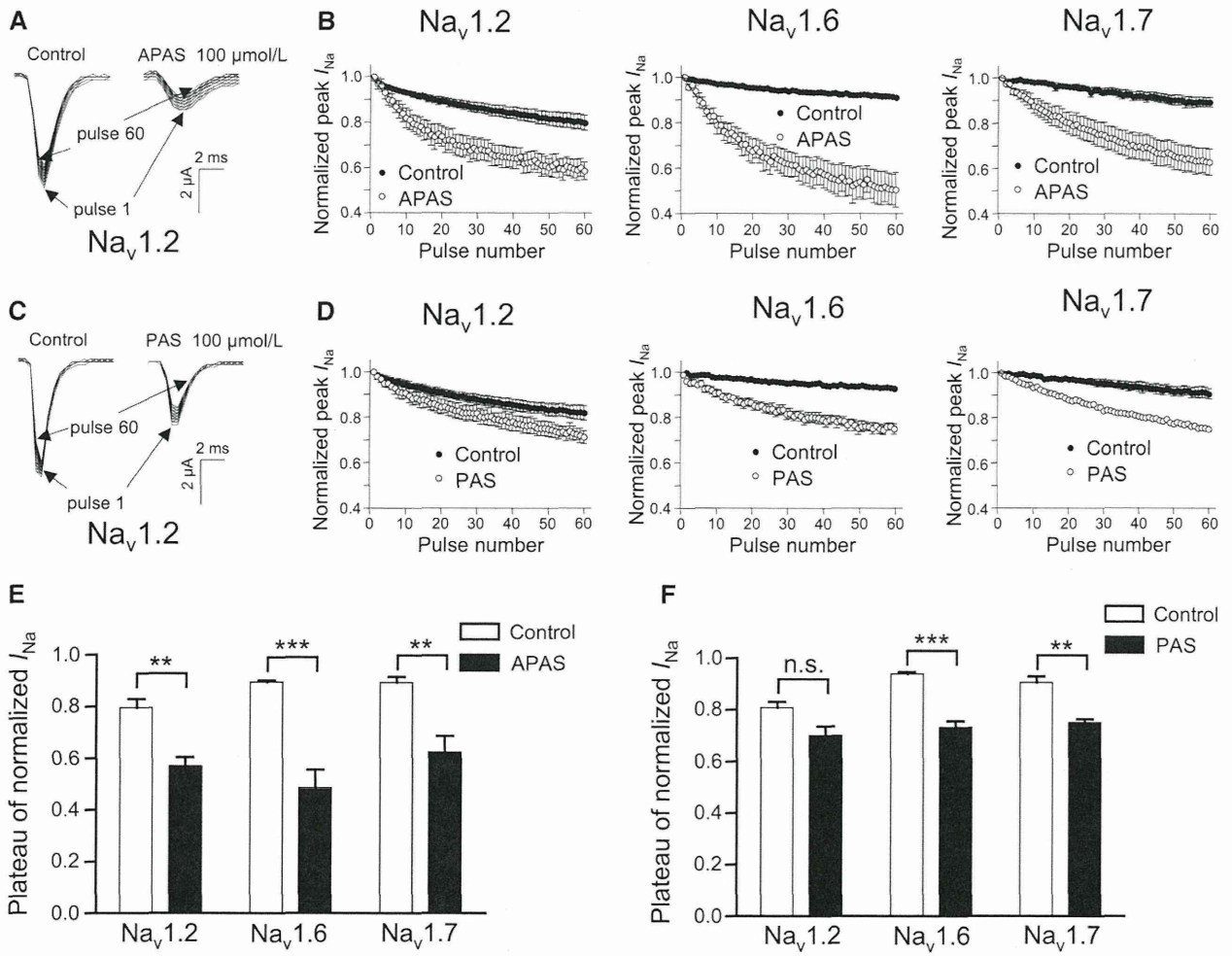

Fig. 8. Use-dependent blockage of sodium channels on Na$_v$1.2 (n = 5), Na$_v$1.6 (n = 6), and Na$_v$1.7 (n = 5) α subunits with β_1 subunits by allopregnanolone sulfate (APAS) and pregnanolone sulfate (PAS). Currents were elicited at 10 Hz by a 20-ms depolarizing pulse of –20 mV for Na$_v$1.2 and Na$_v$1.6 and –10 mV for Na$_v$1.7 from a $V_{1/2}$ holding potential in both the absence and presence of 100 μmol/l of the two compounds; representative I_{Na} traces in both the absence and presence of the two compounds (*A* and *C*). Peak currents were measured and normalized to the first pulse and plotted against the pulse number (*B*, the effects of APAS; *D*, the effects of PAS). *Closed circles* and *open circles* represent control and the effect of neurosteroids, respectively. Data were fitted to the monoexponential equation, and values for fractional blockage of the plateau of normalized I_{Na} are shown in *E* and *F*. Data are expressed as means ± SEM. $^{**}P < 0.01$ and $^{***}P < 0.001$ compared with the control, based on paired *t* test (two-tailed). Na$_v$ = voltage-gated sodium channel.

allopregnanolone shows analgesic effects in rats through suppression of T-type Ca^{2+} currents and potentiation of $GABA_A$ currents.[16] These previous reports indicate several mechanisms underlying the analgesic effect of allopregnanolone likely exist, as well as potentiation of $GABA_A$ receptors.

Sodium channel α subunits expressed in the dorsal root ganglion (Na$_v$1.7, Na$_v$1.8, and Na$_v$1.9) are thought to be involved in the pathogenesis of inflammatory and neuropathic pain. A recent study reported that Na$_v$1.2 also plays an important role in pain signaling. It was reported that Na$_v$1.2 and Na$_v$1.3 predominantly compose functional sodium channel currents within lamina I/II (dorsal horn) neurons, which mediate acute and chronic nociceptive signals from peripheral nociceptors to pain-processing regions in the brain.[37] Another recent report showed that mutations in Na$_v$1.2 are associated with seizures and pain characterized by headaches and back pain.[38] A disubstituted succinamide, a potent sodium channel blocker, was reported to attenuate nociceptive behavior in a rat model of tonic pain and was demonstrated to potently block Na$_v$1.2, as well as Na$_v$1.7 and Na$_v$1.8, with a potency two orders of magnitude higher than anticonvulsant and antiarrhythmic sodium channel blockers currently used to treat neuropathic pain.[39] Other investigators demonstrated that four sodium channel blockers, including lidocaine, mexiletine, benzocaine, and ambroxol, which are used clinically to treat pain, suppressed recombinant Na$_v$1.2 currents as well as tetrodotoxin-resistant Na^+ channel currents in rat sensory neurons, which comprised mostly Na$_v$1.8 currents. The authors suggested that these sodium channel blockers would induce analgesia according

to the amount of sodium channel blocking, including $Na_v1.2$ and $Na_v1.8$.[40] These recent reports support that suppression of $Na_v1.2$ function by APAS might be a mechanism underlying the analgesic effects of allopregnanolone.

In conclusion, APAS and PAS have diverse effects on $Na_v1.2$, $Na_v1.6$, $Na_v1.7$, and $Na_v1.8$ α subunits expressed in *Xenopus* oocytes, with differences in the effects on sodium channel gating. In particular, only APAS inhibited sodium currents of $Na_v1.2$ at pharmacologically relevant concentrations. These results raise the possibility that suppression of $Na_v1.2$ by APAS may be important for pain relief by allopregnanolone and provide a better understanding of the mechanisms underlying the analgesic effects of allopregnanolone. However, further studies are needed to clarify the relevance of sodium channel inhibition by APAS.

Acknowledgments

This study was supported by a Grant-in-Aid for Scientific Research from the Japan Society for the Promotion of Science, Tokyo, Japan (grant no. 21791480 to Dr. Horishita).

Competing Interests

The authors declare no competing interests.

Correspondence

Address correspondence to Dr. Horishita: Department of Anesthesiology, School of Medicine, University of Occupational and Environmental Health, 1-1 Isegaoka, Yahatanisiku, Kitakyushu 807–8555, Japan. thori@med.uoeh-u.ac.jp.

References

1. Baulieu EE: Neurosteroids: A novel function of the brain. Psychoneuroendocrinology 1998; 23:963–87
2. Compagnone NA, Mellon SH: Neurosteroids: Biosynthesis and function of these novel neuromodulators. Front Neuroendocrinol 2000; 21:1–56
3. Morrow AL: Recent developments in the significance and therapeutic relevance of neuroactive steroids—Introduction to the special issue. Pharmacol Ther 2007; 116:1–6
4. Brinton RD: Neurosteroids as regenerative agents in the brain: Therapeutic implications. Nat Rev Endocrinol 2013; 9:241–50
5. Majewska MD, Harrison NL, Schwartz RD, Barker JL, Paul SM: Steroid hormone metabolites are barbiturate-like modulators of the GABA receptor. Science 1986; 232:1004–7
6. Van Hemelrijck J, Muller P, Van Aken H, White PF: Relative potency of eltanolone, propofol, and thiopental for induction of anesthesia. ANESTHESIOLOGY 1994; 80:36–41
7. Zhu D, Wang MD, Bäckström T, Wahlström G: Evaluation and comparison of the pharmacokinetic and pharmacodynamic properties of allopregnanolone and pregnanolone at induction of anaesthesia in the male rat. Br J Anaesth 2001; 86:403–12
8. Kavaliers M, Wiebe JP: Analgesic effects of the progesterone metabolite, 3α-hydroxy-5α-pregnan-20-one, and possible modes of action in mice. Brain Res 1987; 415:393–8
9. Pathirathna S, Todorovic SM, Covey DF, Jevtovic-Todorovic V: 5α-Reduced neuroactive steroids alleviate thermal and mechanical hyperalgesia in rats with neuropathic pain. Pain 2005; 117:326–39
10. Ocvirk R, Pearson Murphy BE, Franklin KB, Abbott FV: Antinociceptive profile of ring A-reduced progesterone metabolites in the formalin test. Pain 2008; 138:402–9
11. Meyer L, Patte-Mensah C, Taleb O, Mensah-Nyagan AG: Allopregnanolone prevents and suppresses oxaliplatin-evoked painful neuropathy: Multi-parametric assessment and direct evidence. Pain 2011; 152:170–81
12. Kawano T, Soga T, Chi H, Eguchi S, Yamazaki F, Yokoyama M: The involvement of the neurosteroid allopregnanolone in the antihyperalgesic effect of paroxetine in a rat model of neuropathic pain. Neuroreport 2011; 22:984–8
13. Sasso O, Russo R, Vitiello S, Raso GM, D'Agostino G, Iacono A, Rana GL, Vallée M, Cuzzocrea S, Piazza PV, Meli R, Calignano A: Implication of allopregnanolone in the antinociceptive effect of *N*-palmitoylethanolamide in acute or persistent pain. Pain 2012; 153:33–41
14. Aouad M, Petit-Demoulière N, Goumon Y, Poisbeau P: Etifoxine stimulates allopregnanolone synthesis in the spinal cord to produce analgesia in experimental mononeuropathy. Eur J Pain 2014; 18:258–68
15. Jasmin L, Wu MV, Ohara PT: GABA puts a stop to pain. Curr Drug Targets CNS Neurol Disord 2004; 3:487–505
16. Pathirathna S, Brimelow BC, Jagodic MM, Krishnan K, Jiang X, Zorumski CF, Mennerick S, Covey DF, Todorovic SM, Jevtovic-Todorovic V: New evidence that both T-type calcium channels and $GABA_A$ channels are responsible for the potent peripheral analgesic effects of 5α-reduced neuroactive steroids. Pain 2005; 114:429–43
17. Kussius CL, Kaur N, Popescu GK: Pregnanolone sulfate promotes desensitization of activated NMDA receptors. J Neurosci 2009; 29:6819–27
18. Catterall WA: From ionic currents to molecular mechanisms: The structure and function of voltage-gated sodium channels. Neuron 2000; 26:13–25
19. Catterall WA, Goldin AL, Waxman SG: International Union of Pharmacology. XLVII. Nomenclature and structure-function relationships of voltage-gated sodium channels. Pharmacol Rev 2005; 57:397–409
20. Wood JN, Boorman JP, Okuse K, Baker MD: Voltage-gated sodium channels and pain pathways. J Neurobiol 2004; 61:55–71
21. Cummins TR, Sheets PL, Waxman SG: The roles of sodium channels in nociception: Implications for mechanisms of pain. Pain 2007; 131:243–57
22. Wang W, Gu J, Li YQ, Tao YX: Are voltage-gated sodium channels on the dorsal root ganglion involved in the development of neuropathic pain? Mol Pain 2011; 7:16
23. Horishita T, Ueno S, Yanagihara N, Sudo Y, Uezono Y, Okura D, Sata T: Inhibition by pregnenolone sulphate, a metabolite of the neurosteroid pregnenolone, of voltage-gated sodium channels expressed in *Xenopus* oocytes. J Pharmacol Sci 2012; 120:54–8
24. Horishita T, Eger EI II, Harris RA: The effects of volatile aromatic anesthetics on voltage-gated Na^+ channels expressed in *Xenopus* oocytes. Anesth Analg 2008; 107:1579–86
25. Scholz A, Kuboyama N, Hempelmann G, Vogel W: Complex blockade of TTX-resistant Na+ currents by lidocaine and bupivacaine reduce firing frequency in DRG neurons. J Neurophysiol 1998; 79:1746–54
26. Driscoll WJ, Martin BM, Chen HC, Strott CA: Isolation of two distinct 3-hydroxysteroid sulfotransferases from the guinea pig adrenal. Evidence for 3α-hydroxy *versus* 3 β-hydroxy stereospecificity. J Biol Chem 1993; 268:23496–503
27. Schlichter R, Keller AF, De Roo M, Breton JD, Inquimbert P, Poisbeau P: Fast nongenomic effects of steroids on synaptic

transmission and role of endogenous neurosteroids in spinal pain pathways. J Mol Neurosci 2006; 28:33–51

28. Mellon SH: Neurosteroid regulation of central nervous system development. Pharmacol Ther 2007; 116:107–24
29. Charlet A, Lasbennes F, Darbon P, Poisbeau P: Fast non-genomic effects of progesterone-derived neurosteroids on nociceptive thresholds and pain symptoms. Pain 2008; 139:603–9
30. Kawano T, Soga T, Chi H, Eguchi S, Yamazaki F, Kumagai N, Yokoyama M: Role of the neurosteroid allopregnanolone in the hyperalgesic behavior induced by painful nerve injury in rats. J Anesth 2011; 25:942–5
31. Akk G, Li P, Bracamontes J, Reichert DE, Covey DF, Steinbach JH: Mutations of the $GABA_A$ receptor α1 subunit M1 domain reveal unexpected complexity for modulation by neuroactive steroids. Mol Pharmacol 2008; 74:614–27
32. Lambert JJ, Belelli D, Harney SC, Peters JA, Frenguelli BG: Modulation of native and recombinant $GABA_A$ receptors by endogenous and synthetic neuroactive steroids. Brain Res Brain Res Rev 2001; 37:68–80
33. Wang GK, Russell C, Wang SY: State-dependent block of voltage-gated Na^+ channels by amitriptyline *via* the local anesthetic receptor and its implication for neuropathic pain. Pain 2004; 110:166–74
34. Ragsdale DS, McPhee JC, Scheuer T, Catterall WA: Molecular determinants of state-dependent block of Na^+ channels by local anesthetics. Science 1994; 265:1724–8
35. Poyraz D, Bräu ME, Wotka F, Puhlmann B, Scholz AM, Hempelmann G, Kox WJ, Spies CD: Lidocaine and octanol have different modes of action at tetrodotoxin-resistant Na^+ channels of peripheral nerves. Anesth Analg 2003; 97:1317–24
36. Ouyang W, Herold KF, Hemmings HC Jr: Comparative effects of halogenated inhaled anesthetics on voltage-gated Na^+ channel function. ANESTHESIOLOGY 2009; 110:582–90
37. Hildebrand ME, Mezeyova J, Smith PL, Salter MW, Tringham E, Snutch TP: Identification of sodium channel isoforms that mediate action potential firing in lamina I/II spinal cord neurons. Mol Pain 2011; 7:67
38. Liao Y, Anttonen AK, Liukkonen E, Gaily E, Maljevic S, Schubert S, Bellan-Koch A, Petrou S, Ahonen VE, Lerche H, Lehesjoki AE: SCN2A mutation associated with neonatal epilepsy, late-onset episodic ataxia, myoclonus, and pain. Neurology 2010; 75:1454–8
39. Priest BT, Garcia ML, Middleton RE, Brochu RM, Clark S, Dai G, Dick IE, Felix JP, Liu CJ, Reiseter BS, Schmalhofer WA, Shao PP, Tang YS, Chou MZ, Kohler MG, Smith MM, Warren VA, Williams BS, Cohen CJ, Martin WJ, Meinke PT, Parsons WH, Wafford KA, Kaczorowski GJ: A disubstituted succinamide is a potent sodium channel blocker with efficacy in a rat pain model. Biochemistry 2004; 43:9866–76
40. Weiser T: Comparison of the effects of four Na^+ channel analgesics on TTX-resistant Na^+ currents in rat sensory neurons and recombinant $Na_v1.2$ channels. Neurosci Lett 2006; 395:179–84

The Endocannabinoid Anandamide Inhibits Voltage-Gated Sodium Channels $Na_v1.2$, $Na_v1.6$, $Na_v1.7$, and $Na_v1.8$ in *Xenopus* Oocytes

Dan Okura, MD,* Takafumi Horishita, MD, PhD,* Susumu Ueno, MD, PhD,† Nobuyuki Yanagihara, PhD,† Yuka Sudo, PhD,§ Yasuhito Uezono, MD, PhD,‖ and Takeyoshi Sata, MD, PhD*

BACKGROUND: Anandamide is an endocannabinoid that regulates multiple physiological functions by pharmacological actions, in a manner similar to marijuana. Recently, much attention has been paid to the analgesic effect of endocannabinoids in terms of identifying new pharmacotherapies for refractory pain management, but the mechanisms of the analgesic effects of anandamide are still obscure. Voltage-gated sodium channels are believed to play important roles in inflammatory and neuropathic pain. We investigated the effects of anandamide on 4 neuronal sodium channel α subunits, $Na_v1.2$, $Na_v1.6$, $Na_v1.7$, and $Na_v1.8$, to explore the mechanisms underlying the antinociceptive effects of anandamide.

METHODS: We studied the effects of anandamide on $Na_v1.2$, $Na_v1.6$, $Na_v1.7$, and $Na_v1.8$ α subunits with β_1 subunits by using whole-cell, 2-electrode, voltage-clamp techniques in *Xenopus* oocytes.

RESULTS: Anandamide inhibited sodium currents of all subunits at a holding potential causing half-maximal current ($V_{1/2}$) in a concentration-dependent manner. The half-maximal inhibitory concentration values for $Na_v1.2$, $Na_v1.6$, $Na_v1.7$, and $Na_v1.8$ were 17, 12, 27, and 40 μmol/L, respectively, indicating an inhibitory effect on $Na_v1.6$, which showed the highest potency. Anandamide raised the depolarizing shift of the activation curve as well as the hyperpolarizing shift of the inactivation curve in all α subunits, suggesting that sodium current inhibition was due to decreased activation and increased inactivation. Moreover, anandamide showed a use-dependent block in $Na_v1.2$, $Na_v1.6$, and $Na_v1.7$ but not $Na_v1.8$.

CONCLUSION: Anandamide inhibited the function of α subunits in neuronal sodium channels $Na_v1.2$, $Na_v1.6$, $Na_v1.7$, and $Na_v1.8$. These results help clarify the mechanisms of the analgesic effects of anandamide. (Anesth Analg 2014;118:554–62)

Cannabis has been used as a pleasure-inducing drug and traditional medicine for thousands of years, and since the 2 cannabinoid receptors CB_1[1,2] and CB_2[3] were identified, the endocannabinoid signaling system has been a focus of medical research and has been considered a potential therapeutic target.[4] Endocannabinoids mimic the pharmacological actions of the psychoactive principle agent in marijuana, Δ^9-tetrahydrocannabinol, and regulate multiple physiological functions, such as analgesia, regulation of food intake, immunomodulation, inflammation, addictive behavior, epilepsy, and others.[5]

Anandamide, the ethanolamide of arachidonic acid, was the first endocannabinoid isolated from the brain[6]; it acts as a partial agonist on CB_1 receptors, with a lesser effect on CB_2 receptors.[7] Several groups have shown an analgesic effect of exogenous anandamide through the CB_1 receptor in acute,[8–10] persistent inflammatory,[11–13] and neuropathic pain models.[14,15] CB_1 receptors are distributed throughout the pain pathways of the central nervous system (CNS), including the periaqueductal gray, amygdala, and spinal trigeminal tract,[16,17] and the peripheral nervous system including the dorsal root ganglion (DRG),[18] suggesting an analgesic effect of anandamide via CB_1 receptors. However, anandamide may also act on other ion channels consisting of pain signaling pathways, including voltage-gated Ca^{2+} channels, TASK1 channels, 5-HT_3 receptor, rectifying K^+ channels, and N-methyl-D-aspartate receptors[19–24]; thus, the mechanisms of the analgesic effects of anandamide remain unclear.

Voltage-gated sodium channels play an essential role in action potential initiation and propagation in excitable nerve and muscle cells. Nine distinct pore-forming α subunits ($Na_v1.1$–$Na_v1.9$), which are associated with auxiliary β subunits, have been identified,[25,26] and each has a different pattern of development and localization as well as distinct physiological and pathophysiological roles. Sodium channel α subunits expressed in DRG ($Na_v1.7$, $Na_v1.8$, $Na_v1.9$) are believed to play crucial roles in inflammatory and neuropathic pain and are considered potential targets of these conditions.[27–30] Previous studies have shown that anandamide inhibits sodium channel function in the brain through the inhibition of veratridine-dependent depolarization of synaptosomes[31] and suppresses tetrodotoxin-sensitive (TTX-S) and tetrodotoxin-resistant (TTX-R) sodium currents in rat

From the *Department of Anesthesiology, School of Medicine; †Department of Occupational Toxicology, Institute of Industrial Ecological Sciences, University of Occupational and Environmental Health, ‡Department of Pharmacology, School of Medicine, University of Occupational and Environmental Health, Fukuoka; §Department of Molecular Pathology & Metabolic Disease, Faculty of Pharmaceutical Sciences, Tokyo university of Science, Chiba; and ‖Cancer Pathophysiology Division, National Cancer Center Research Institute, Tokyo, Japan.

Accepted for publication November 15, 2013.

Funding: This study was supported by a Grant-in-Aid for Scientific Research from the Ministry of Education, Culture, Sports, Science and Technology, 24592369 (to T.H.).

The authors declare no conflicts of interest.

Reprints will not be available from the authors.

Address correspondence to Takafumi Horishita, MD, PhD, Department of Anesthesiology, School of Medicine, University of Occupational and Environmental Health, 1-1 Iseigaoka, Yahatanishiku, Kitakyushu, Fukuoka 807–8555, Japan. Address e-mail to thori@med.uoeh-u.ac.jp.

DOI: 10.1213/ANE.0000000000000070

DRG neurons.[32] These results suggest that sodium channels are potential targets for anandamide. However, the precise mechanisms of anandamide on each α subunit are still unknown. It is of great importance to clarify these mechanisms because each α subunit has a difference of 20% to 50% in amino acid sequence in the transmembrane and extracellular domains and therefore has different physiological functions. Here, we explored the effects of anandamide on several sodium channel α subunits, including $Na_v1.2$, that is expressed primarily in the CNS; $Na_v1.6$ that is expressed in the CNS and DRG neurons; and $Na_v1.7$ and $Na_v1.8$ that are expressed in DRG neurons.

METHODS

This study was approved by the Animal Research Committee of the University of Occupational and Environmental Health.

Materials

Adult female *Xenopus laevis* frogs were obtained from Kyudo Co., Ltd. (Saga, Japan). Anandamide was purchased from Sigma-Aldrich (St. Louis, MO). Rat $Na_v1.2$ α subunit cDNA was a gift from Dr. W. A. Catterall (University of Washington, Seattle, WA). Rat $Na_v1.6$ α subunit cDNA was a gift from Dr. A. L. Goldin (University of California, Irvine, CA). Rat $Na_v1.7$ α subunit cDNA was a gift from G. Mandel (Oregon Health and Science University, Portland, OR). Rat $Na_v1.8$ α subunit cDNA was a gift from Dr. A. N. Akopian (University of Texas Health Science Center, San Antonio, TX), and human β_1 subunit cDNA was a gift from Dr. A. L. George (Vanderbilt University, Nashville, TN).

cRNA Preparation and Oocyte Injection

After linearization of cDNA with *Cla*I ($Na_v1.2$ α subunit), *Not*I ($Na_v1.6$, 1.7 α subunit), *Xba*I ($Na_v1.8$ α subunit), and *EcoR*I (β_1 subunit), cRNAs were transcribed by using SP6 (1.8 α, β_1 subunit) or T7 ($Na_v1.2$, 1.6 1.7 α subunit) RNA polymerase from the mMESSAGE mMACHINE kit (Ambion, Austin, TX). Preparation of *X. laevis* oocytes and cRNA microinjection were performed as described previously.[33] Briefly, stage IV to VI oocytes were manually isolated from a removed portion of ovary. Next, oocytes were treated with collagenase (0.5 mg/mL) for 10 minutes and placed in modified Barth's solution (88 mmol/L NaCl, 1 mmol/L KCl, 2.4 mmol/L $NaHCO_3$, 10 mmol/L HEPES, 0.82 mmol/L $MgSO_4$, 0.33 mmol/L $Ca(NO_3)_2$, and 0.91 mmol/L $CaCl_2$, adjusted to pH 7.5), supplemented with 10,000 U penicillin, 50 mg gentamicin, 90 mg theophylline, and 220 mg sodium pyruvate per liter (incubation medium). Na_v α subunit cRNAs were coinjected with β_1 subunit cRNA at a ratio of 1:10 (total volume was 20–40 ng/50 nL) into *Xenopus* oocytes (all α subunits were coinjected with the β_1 subunit). Injected oocytes were incubated at 19°C in incubation medium, and 2 to 6 days after injection, the cells were used for electrophysiological recordings.

Electrophysiological Recordings

All electrical recordings were performed at room temperature (23°C). Oocytes were placed in a 100 μL recording chamber and perfused at 2 mL/min with Frog Ringer's solution containing 115 mmol/L NaCl, 2.5 mmol/L KCl, 10 mmol/L HEPES, 1.8 mmol/L $CaCl_2$, pH 7.2, by using a peristaltic pump (World Precision Instruments Inc., Sarasota, FL). Recording electrodes were prepared with borosilicate glass by using a puller (PP-830, Narishige group company, Tokyo, Japan), and microelectrodes were filled with 3 mol KCl/0.5% low-melting-point agarose with resistances between 0.3 and 0.5 MΩ. The whole-cell voltage clamp was achieved through these 2 electrodes by using a Warner Instruments model OC-725C (Warner, Hamden, CT). Currents were recorded and analyzed by using pCLAMP 7.0 software (Axon Instruments, Foster City, CA), and the amplitude of expressed sodium currents was typically 2 to 15 μA. Transients and leak currents were subtracted by using the P/N procedure. Anandamide stocks were prepared in dimethylsulphoxide (DMSO) and diluted in Frog Ringer's solution to a final DMSO concentration not exceeding 0.05%. Anandamide was then perfused for 5 to 10 minutes to reach equilibrium.

The voltage dependence of activation was determined by using 50-millisecond depolarizing pulses from a holding potential causing maximal current, V_{max} (–90 mV for $Na_v1.2$ and $Na_v1.6$ or –100 mV for $Na_v1.7$ and $Na_v1.8$), and from a holding potential causing half-maximal current, $V_{1/2}$ (from approximately –40 mV to –70 mV) to 50 mV in 10 mV increments. Normalized activation curves were fitted to the Boltzmann equation: $G/G_{max} = 1/(1 + \exp(V_{1/2} - V)/k)$, where G is the voltage-dependent sodium conductance, G_{max} is the maximal sodium conductance, G/G_{max} is the normalized fractional conductance, $V_{1/2}$ is the potential at which activation is half maximal, and k is the slope factor. The G value for each oocyte was calculated by using the formula $G = I/(Vt - Vr)$, where I is the peak sodium current, Vt is the test potential and Vr is the reversal potential. The Vr for each oocyte was estimated by extrapolating the linear ascending segment of the current voltage relationship (I–V) curve to the voltage axis. To measure steady-state inactivation, currents were elicited by a 50-millisecond test pulse to –20 mV for $Na_v1.2$ and $Na_v1.6$ or –10 mV for $Na_v1.7$ or +10 mV for $Na_v1.8$ after 200 milliseconds (500 milliseconds for only $Na_v1.8$) prepulses ranging from –140 mV to 0 mV in 10 mV increments from a holding potential of V_{max}. Steady-state inactivation curves were fitted to the Boltzmann equation: $I/I_{max} = 1/(1 + \exp(V_{1/2} - V)/k)$, where I_{max} is the maximal sodium current, I/I_{max} is the normalized current, $V_{1/2}$ is the voltage of half-maximal inactivation, and k is the slope factor. To investigate a use-dependent sodium channel block of anandamide, currents were elicited at 10 Hz by a 20-millisecond depolarizing pulse of –20 mV for $Na_v1.2$ and $Na_v1.6$ or –10 mV for $Na_v1.7$ or +10 mV for $Na_v1.8$ from a $V_{1/2}$ holding potential in both the absence and presence of 30 μmol/L anandamide. Peak currents were measured and normalized to the first pulse and plotted against the pulse number. Data were fitted to the monoexponential equation $I_{Na} = \exp(-\tau_{use} \cdot n) + C$, where n is pulse number, C is the plateau I_{Na}, and τ_{use} is the time constant of use-dependent decay.

Data Analysis

All values are presented as the mean ± SEM (n = 5–8). The n values refer to the number of oocytes examined. Each experiment was performed with oocytes from at least 2 frogs.

Control sodium current recorded in absence of anandamide was assigned a value of 100%. Data were statistically evaluated by paired *t* test by using GraphPad Prism software (GraphPad Software, Inc., San Diego, CA). Hill slope and half-maximal inhibitory concentration values were also calculated by using this software.

RESULTS

Effects of Anandamide on Peak Na+ Inward Currents

Currents were elicited by using a 50-millisecond depolarizing pulse to –20 mV for $Na_v1.2$ and $Na_v1.6$ or –10 mV for $Na_v1.7$ or +10 mV for $Na_v1.8$ applied every 10 seconds from V_{max} or $V_{1/2}$ holding potential in both the absence and presence of 10 μmol/L anandamide (Fig. 1); anandamide was applied for 10 minutes. Anandamide inhibited the peak I_{Na} induced by all α subunits more potently at $V_{1/2}$ than V_{max}. Anandamide reduced the peak I_{Na} induced by $Na_v1.2$, $Na_v1.6$, $Na_v1.7$, and $Na_v1.8$ by 46 ± 4, 49 ± 3, 37 ± 2, and 27 ± 2 at $V_{1/2}$, respectively, and 7 ± 2, 6 ± 1, 9 ± 1, and 21 ± 5% at V_{max}, respectively (Fig. 2). Inhibition of anandamide at $V_{1/2}$ was statistically significant in all α subunits, but those at V_{max} were not statistically significant except for the suppression in $Na_v1.8$ by paired *t* test. Because suppression at $V_{1/2}$ was potent, we examined the concentration-response relation for anandamide inhibition of the peak I_{Na} induced by $Na_v1.2$, $Na_v1.6$, $Na_v1.7$, and $Na_v1.8$ at $V_{1/2}$ holding potential (Fig. 3). The peak current amplitude in the presence of anandamide was normalized to that in the control, and the effects of anandamide were expressed as percentages of the control. Nonlinear regression analyses of the dose-response curves yielded half-maximal inhibitory concentration values and Hill slopes of 17 ± 3 μmol/L and 0.74 ± 0.04 for $Na_v1.2$, 12 ± 1 μmol/L and 0.79 ± 0.08 for $Na_v1.6$, 27 ± 3 μmol/L and 0.52 ± 0.06 for $Na_v1.7$, 40 ± 14 μmol/L and 0.71 ± 0.10 for $Na_v1.8$, respectively (Fig. 3).

Effects of Anandamide on Sodium Current Activation

We examined the effects of anandamide on 4 α subunits of sodium current activation. Voltage dependence of activation was determined by using 50-millisecond depolarizing pulses from a holding potential of V_{max} to 50 mV in 10 mV increments or from a holding potential of $V_{1/2}$ to 50 mV in 10 mV increments for $Na_v1.2$, $Na_v1.6$, $Na_v1.7$, and $Na_v1.8$. Activation curves were derived from the I-V curves (see Methods); anandamide (30 μmol/L) was applied for 5 minutes. The peak I_{Na} was reduced by anandamide at V_{max} and $V_{1/2}$ holding potentials with all subunits (Fig. 4). Anandamide shifted the midpoint of steady-state activation ($V_{1/2}$) in a depolarizing direction at both holding potentials for all subunits (Fig. 5). These shifts were small (1.9–3.8 mV) but statistically significant (Table 1).

Effects of Anandamide on Sodium Current Inactivation

The effect of anandamide on steady-state inactivation was also investigated. Currents were elicited by a 50-millisecond test pulse to –20 mV for $Na_v1.2$ and $Na_v1.6$ or –10 mV for $Na_v1.7$ or +10 mV for $Na_v1.8$ after 200 millis econds(500 milliseconds for only $Na_v1.8$) prepulses ranging from –140 mV to 0 mV in 10 mV increments from a holding potential of V_{max}. Steady-state inactivation curves were fitted to the Boltzmann equation (see Methods); anandamide (30 μmol/L) was applied for 5 minutes. Anandamide significantly shifted the midpoint of steady-state inactivation ($V_{1/2}$) in the hyperpolarizing direction by 5.2, 5.0, 4.1, and 6.3 mV in $Na_v1.2$, $Na_v1.6$, $Na_v1.7$, and $Na_v1.8$, respectively (Fig. 6, Table 1).

Use-Dependent Block of Sodium Currents by Anandamide

We investigated the use-dependent block of sodium currents by anandamide. Currents were elicited at 10 Hz by a 20-millisecond depolarizing pulse of –20 mV for $Na_v1.2$ and $Na_v1.6$ or –10 mV for $Na_v1.7$ or +10 mV for $Na_v1.8$ from a $V_{1/2}$ holding potential in both the absence and presence of 30 μmol/L anandamide. Peak currents were measured and normalized to the first pulse and plotted against the pulse number (Fig. 7, A–D). Data were fitted by the monoexponential equation (see Methods); anandamide was applied for 5 minutes. Anandamide significantly reduced the plateau I_{Na} amplitude of $Na_v1.2$, $Na_v1.6$, and $Na_v1.7$ from 0.74 ± 0.02 to 0.66 ± 0.03, 0.88 ± 0.01 to 0.66 ± 0.02, and 0.73 ±

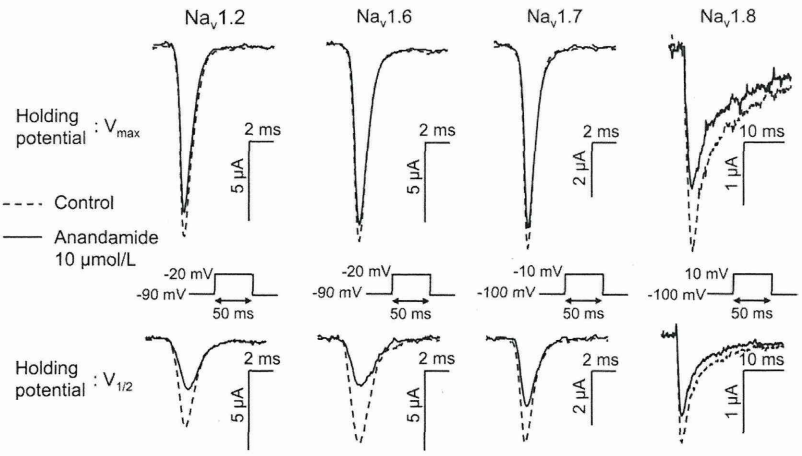

Figure 1. Inhibitory effects of anandamide on peak sodium inward currents in *Xenopus* oocytes expressing $Na_v1.2$, $Na_v1.6$, $Na_v1.7$, and $Na_v1.8$ α subunits with β_1 subunits at 2 holding potentials. Representative traces are shown. Sodium currents were evoked by 50-millisecond depolarizing pulses to –20 mV for $Na_v1.2$ and $Na_v1.6$ or –10 mV for $Na_v1.7$ or +10 mV for $Na_v1.8$ from V_{max} holding potential (upper panel) or $V_{1/2}$ holding potential (lower panel) in both the absence and presence of 10 μmol/L anandamide; anandamide was applied for 10 minutes.

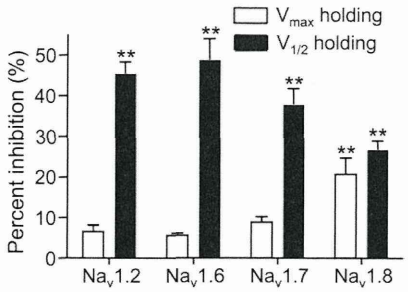

Figure 2. Inhibitory effects of anandamide on peak sodium inward currents in *Xenopus* oocytes expressing $Na_v1.2$, $Na_v1.6$, $Na_v1.7$, and $Na_v1.8$ α subunits with β_1 subunits at 2 holding potentials. Percent inhibition of sodium current of anandamide was calculated. Open columns represent the effect at V_{max} holding potential, and closed columns indicate the effect at $V_{1/2}$ holding potential. Anandamide inhibited the peak I_{Na} induced by $Na_v1.2$, $Na_v1.6$, $Na_v1.7$, and $Na_v1.8$ by 46 ± 4, 49 ± 3, 37 ± 2, and 27 ± 2 at $V_{1/2}$, respectively, and 7 ± 2, 6 ± 1, 9 ± 1, and 21 ± 5% at V_{max}, respectively. Data are represented as the mean ± SEM (n = 5–7). $^{**}P < 0.01$, compared with the control (based on paired t test).

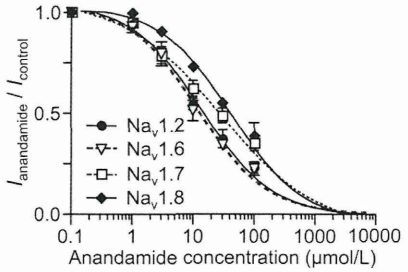

Figure 3. Concentration-response curves for anandamide suppression of sodium currents elicited by 50-millisecond depolarizing pulses to –20 mV for $Na_v1.2$ and $Na_v1.6$ or –10 mV for $Na_v1.7$ or +10 mV for $Na_v1.8$ from $V_{1/2}$ holding potential. The peak current amplitude in the presence of anandamide was normalized to that in the control, and the effects of anandamide are expressed as percentages of the control. Half-maximal inhibitory concentration values and Hill slopes were 17 ± 3 μmol/L and 0.74 ± 0.04 for $Na_v1.2$, 12 ± 1 μmol/L and 0.79 ± 0.08 for $Na_v1.6$, 27 ± 3 μmol/L and 0.52 ± 0.06 for $Na_v1.7$, and 40 ± 14 μmol/L and 0.71 ± 0.10 for $Na_v1.8$, respectively. Data are represented as the mean ± SEM (n = 5–8). Data were fit to the Hill slope equation to give the half-maximal inhibitory concentration values and Hill slopes. Half-maximal inhibitory concentration values and Hill slopes were calculated by using GraphPad Prism.

0.03 to 0.57 ± 0.04, respectively (Fig. 7E), demonstrating a use-dependent block, whereas anandamide did not reduce the plateau I_{Na} amplitude of $Na_v1.8$ (from 0.86 ± 0.03 to 0.84 ± 0.04).

DISCUSSION

In the present study, we demonstrated that anandamide suppresses the $Na_v1.2$, $Na_v1.6$, $Na_v1.7$, and $Na_v1.8$ α subunits in a concentration-dependent manner. half-maximal inhibitory concentration values ranged from 12 μmol/L ($Na_v1.6$) to 40 μmol/L ($Na_v1.8$). Wiley et al.[34] have reported that IV administration of anandamide produce a dose-dependent antinociceptive effect in the tail-flick test with mice, and the 50% effective dose (ED_{50}) of that was 15 mg/kg. They also have shown that the plasma concentration of anandamide was 4.96 μg/mL (14.3 μmol/L) when 10 mg/kg of anandamide was administered, suggesting that half-maximal inhibitory concentration values used in the present study are pharmacologically relevant and are close to the plasma concentration exhibiting an antinociceptive effect by anandamide. We also demonstrated that anandamide has more potent inhibitory effects on sodium currents at $V_{1/2}$ holding potential (inactivated state) than at V_{max} holding potential (resting state) in a manner similar to that of local anesthetics on sodium channels. Therefore, the analgesic effects of anandamide may be mediated through sodium channel blockade. The present results are partially consistent with previous reports that anandamide suppresses TTX-S veratridine-dependent depolarization of synaptosomes, the binding of batrachotoxin to sodium channels, and TTX-S sustained repetitive firing in cortical neurons[31] and inhibits TTX-S and TTX-R sodium currents in a concentration-dependent manner in rat DRG neurons.[32] However, their precise mechanisms of anandamide on several sodium channel α subunits have not yet been investigated. Considering that $Na_v1.6$ was distributed in both CNS and DRG neurons, and that $Na_v1.8$ was distributed in DRG neurons, our results are consistent with a previous study showing that anandamide inhibited sodium currents with half-maximal inhibitory concentration values of 5.4 μmol/L for the TTX-S current and 38 μmol/L for the TTX-R current in DRG neurons,[32] suggesting that TTX-S and TTX-R currents in DRG neurons may represent $Na_v1.6$ and $Na_v1.8$ currents, respectively. Because $Na_v1.6$ is expressed in both the brain and DRG, and anandamide suppressed $Na_v1.6$ function most potently among the 4 α subunits, the effect of anandamide on $Na_v1.6$ may be the most important.

The effects of anandamide on channel gating, including activation and inactivation, demonstrated common characteristics among the 4 α subunits we studied. Anandamide shifted the midpoint of steady-state activation ($V_{1/2}$) in a depolarizing direction at both $V_{1/2}$ and V_{max} holding potentials for all α subunits, and the shifts were significant, although the shifts were small (approximately 4 mV). Anandamide also significantly shifted the midpoint of steady-state inactivation ($V_{1/2}$) in the hyperpolarizing direction (approximately 7 mV) for all α subunits. These results suggest that both inhibition of activation and the enhancement of inactivation are common mechanisms of sodium current inhibition by anandamide for $Na_v1.2$, $Na_v1.6$, $Na_v1.7$, and $Na_v1.8$. A combination of effects on both activation and inactivation might produce sufficient effects to suppress sodium currents although each effect is small. Inhibition by anandamide at V_{max} holding potential for $Na_v1.2$, $Na_v1.6$, and $Na_v1.7$ was small and not significant, whereas that for $Na_v1.8$ was significant (Fig. 1), indicating that resting-channel block is one of the important mechanisms of anandamide inhibition for only $Na_v1.8$. Anandamide exhibited use-dependent block with repetitive stimuli for $Na_v1.2$, $Na_v1.6$, and $Na_v1.7$ but not $Na_v1.8$. The presence of use-dependent block by anandamide suggests the possibility of open-channel block and the ability to slow the recovery time from blocks that are seen with amitriptyline.[35] Sodium channel blockers such as local anesthetics, tricyclic antidepressants, and volatile anesthetics have been shown to shift the voltage dependence of steady-state inactivation with no effect on

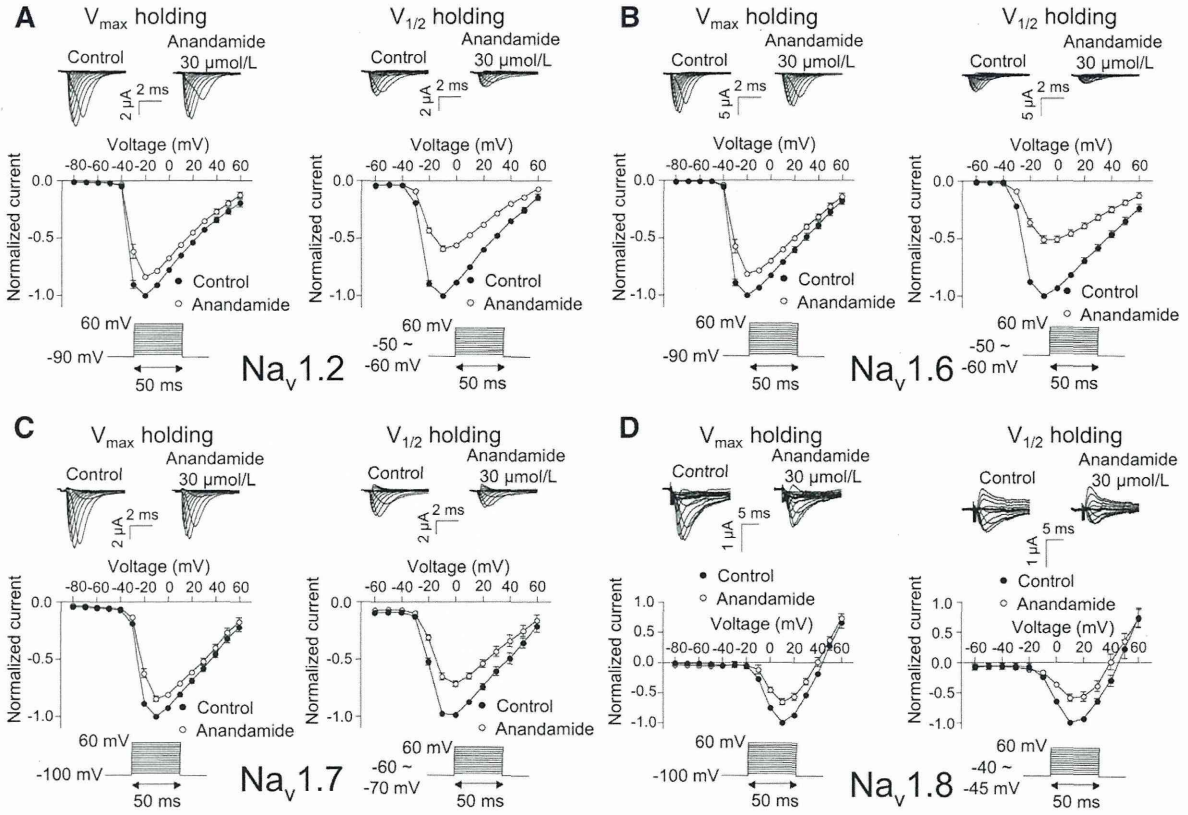

Figure 4. Effects of anandamide on I-V curves of sodium currents in oocytes expressing $Na_v1.2$ (A), $Na_v1.6$ (B), $Na_v1.7$ (C), and $Na_v1.8$ (D) α subunits with β_1 subunits. Currents were elicited by using 50-millisecond depolarizing steps between –80 and 60 mV in 10 mV increments from a V_{max} holding potential (left panel) and elicited by using 50-millisecond depolarizing steps between –60 and 60 mV in 10 mV increments from a $V_{1/2}$ holding potential (right panel); anandamide (30 μmol/L) was applied for 5 minutes; upper panel, representative I_{Na} traces from oocytes expressing $Na_v1.2$, $Na_v1.6$, $Na_v1.7$, and $Na_v1.8$ with β_1 subunits in both the absence and presence of 30 μmol/L anandamide; lower panel, effects of anandamide on representative I-V curves elicited from V_{max} holding potential (left panel) and $V_{1/2}$ holding potential (right panel) (closed circles, control; open circles, anandamide). Peak currents were normalized to the maximal currents observed from –20 to +10 mV. Data are represented as the mean ± SEM (n = 5–8).

activation and exhibit use-dependent block.[35–39] Our results show that anandamide shows a negative shift in the voltage dependence of inactivation and use-dependent block except for $Na_v1.8$ that are seen with other sodium channel blockers yet also shifts the steady-state activation in a depolarizing direction, suggesting that it may have different binding sites or allosteric conformational mechanisms for these sodium channel antagonists. Moreover, a resting-channel block, not an open-channel block, for $Na_v1.8$ may be a key for exploring the mechanism of sodium channel inhibition by anandamide in detail.

Several groups have evaluated antinociception by exogenous anandamide via CB_1 receptors.[8–10] Indeed, a recent review has shown that activation of both CB_1 and CB_2 receptors reduces nociceptive processing in acute and chronic animal models of pain.[40] Alternatively, other investigators have suggested that anandamide produces antinociception through a CB_1-independent mechanism. For example, anandamide antinociception is not blocked by pretreatment with the selective CB_1 antagonist SR141716A.[41] Rapid metabolism of anandamide to arachidonic acid has been shown to be one of the reasons for the failure of SR141716A to antagonize the effects of anandamide; in experiments, the ability of SR141716A to reverse anandamide antinociception was improved (but not completely) when anandamide metabolism to arachidonic acid was inhibited with coadministration of an amidase inhibitor, phenylmethylsulfonyl fluoride.[42] That study also demonstrated that cyclooxygenase did not alter the effects of anandamide, whereas it blocked the effects of arachidonic acid, suggesting a pain-inhibitory effect of anandamide by noncannabinoid mechanisms. Another recent study suggested that anandamide induced antinociception by stimulating endogenous norepinephrine release that activated peripheral adrenoceptors inducing antinociception, although whether the effect was caused through cannabinoid receptors remains unknown.[43]

This study indicates that sodium channel inhibition by anandamide is independent of signaling through cannabinoid receptors, because in recombinant experiments such as our present examination, the effects on channels or receptors can be excluded except for that expressed in membranes. Previous reports also indicate a direct effect of anandamide on sodium channels by demonstrating that sodium channel-related activities by anandamide in the brain may be independent of

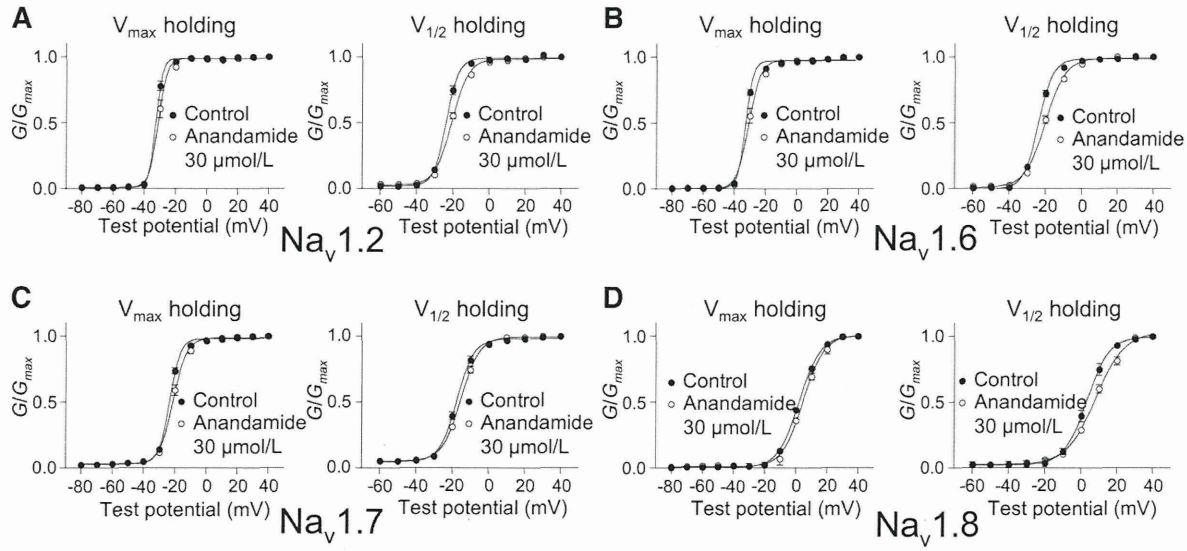

Figure 5. Effects of anandamide on channel activation in oocytes expressing $Na_v1.2$ (A), $Na_v1.6$ (B), $Na_v1.7$ (C), and $Na_v1.8$ (D) α subunits with β_1 subunits from V_{max} holding potential (left panels) or $V_{1/2}$ holding potential (right panels). Closed circles represent control; open circles indicate the effect of anandamide. Data are expressed as the mean ± SEM (n = 5–8). Activation curves were fitted to the Boltzmann equation; $V_{1/2}$ is shown in Table 1.

Table 1. Effects of Anandamide on Activation and Inactivation in Oocytes Expressing $Na_v1.2$, $Na_v1.6$, $Na_v1.7$, and $Na_v1.8$ α Subunits with β_1 Subunits

	$V_{1/2}$ (mV)					
	Holding V_{max}			Holding $V_{1/2}$		
	Control	Anandamide	Shift	Control	Anandamide	Shift
Activation						
$Na_v1.2$	−32.7 ± 0.3	−30.8 ± 0.7*	+1.9	−23.6 ± 0.6	−20.4 ± 0.6**	+3.2
$Na_v1.6$	−32.6 ± 0.3	−30.5 ± 0.7*	+2.1	−23.8 ± 0.5	−20.0 ± 0.6**	+3.8
$Na_v1.7$	−23.4 ± 0.4	−21.0 ± 0.8*	+2.4	−17.3 ± 0.7	−15.0 ± 0.7*	+2.3
$Na_v1.8$	2.2 ± 0.2	4.8 ± 0.8*	+2.6	3.3 ± 1.0	8.4 ± 1.1*	+3.3
Inactivation						
$Na_v1.2$	−51.4 ± 0.7	−56.6 ± 0.8**	−5.2			
$Na_v1.6$	−53.5 ± 0.8	−58.5 ± 1.0**	−5.0			
$Na_v1.7$	−64.3 ± 0.7	−68.4 ± 0.6**	−4.1			
$Na_v1.8$	−50.7 ± 1.4	−57.0 ± 1.9*	−6.3			

*P < 0.05.
**P < 0.01, compared with control (paired t test) (mean ± SEM; n = 5–7).

the presence of AM 251 (a CB_1 antagonist),[31] AM 251, AM 630 (a CB_2 antagonist) and capsazepine (a vanilloid receptor type 1 antagonist) do not interfere with anandamide suppression of sodium currents in DRG.[32] Therefore, we believe that the effects of anandamide on $Na_v1.2$, $Na_v1.6$, $Na_v1.7$, and $Na_v1.8$ α subunits are direct. Taken together, to the best of our knowledge, this is the first direct evidence to demonstrate the inhibitory effects and its mechanisms on neuronal sodium channel α subunits in recombinant experiment systems.

Several sodium channel α subunits are believed to be involved in the pathogenesis of inflammatory and neuropathic pain. Mutations in $Na_v1.7$ have been linked to inherited pain syndromes, including inherited erythromelalgia, that is characterized by episodes of burning pain, erythema, mild swelling in the hands and feet,[44] and paroxysmal extreme pain disorder (PEPD), which is characterized by severe rectal, ocular, and mandibular pain.[45] Recently, anandamide has been reported to inhibit resurgent current of wild-type $Na_v1.7$ and the PEPD mutants expressed in transfected human embryonic kidney 293 cells, and this inhibition was suggested as a therapeutic target for PEPD patients.[46] $Na_v1.8$ has demonstrated its ability to carry most current underlying the upstroke of the action potential in nociceptive neurons,[47] and the use of $Na_v1.8$ knockdown rats after antisense oligodeoxynucleotide treatment has demonstrated a role for $Na_v1.8$ in inflammatory pain,[48] whereas $Na_v1.8$ expression has been reported to increase in nerves proximal to injury sites in patients with chronic neuropathic pain.[49] In an infraorbital nerve injury model of rats, the level of $Na_v1.6$ protein was significantly increased proximal to the lesion site, suggesting a role of $Na_v1.6$ in neuropathic pain conditions.[50] However, these α subunits highly expressed in normal DRG have been reported to show diverse expression in DRG of inflammatory and neuropathic pain models. $Na_v1.7$ mRNA and protein increased in DRG after peripheral inflammation induced by